

Available online at www.sciencedirect.com

ScienceDirect

journal homepage: <http://www.elsevier.com/locate/rpor>

Original research article

Energy spectrum and dose enhancement due to the depth of the Lipiodol position using flattened and unflattened beams



Daisuke Kawahara^{a,b,*}, Shuichi Ozawa^{c,d}, Akito Saito^c, Tomoki Kimura^c,
Tatsuhiko Suzuki^c, Masato Tsuneda^b, Sodai Tanaka^e, Kazunari Hioki^a,
Takeo Nakashima^a, Yoshimi Ohno^a, Yuji Murakami^c, Yasushi Nagata^{c,d}

^a Radiation Therapy Section, Department of Clinical Support, Hiroshima University Hospital, Japan

^b Medical and Dental Sciences Course, Graduate School of Biomedical & Health Sciences, Hiroshima University, Japan

^c Department of Radiation Oncology, Institute of Biomedical & Health Sciences, Hiroshima University, Japan

^d Hiroshima High-Precision Radiotherapy Cancer Center, Japan

^e Department of Nuclear Engineering and Management, School of Engineering, University of Tokyo, Japan

ARTICLE INFO

Article history:

Received 5 July 2017

Received in revised form

24 October 2017

Accepted 27 December 2017

Available online 12 January 2018

Keywords:

Energy spectrum

Lipiodol

Monte Carlo calculation

ABSTRACT

Aim: Lipiodol was used for stereotactic body radiotherapy combining trans arterial chemoembolization. Lipiodol used for tumour seeking in trans arterial chemoembolization remains in stereotactic body radiation therapy. In our previous study, we reported the dose enhancement effect in Lipiodol with 10× flattening-filter-free (FFF). The objective of our study was to evaluate the dose enhancement and energy spectrum of photons and electrons due to the Lipiodol depth with flattened (FF) and FFF beams.

Methods: FF and FFF for 6MV beams from TrueBeam were used in this study. The Lipiodol (3 × 3 × 3 cm³) was located at depths of 1, 3, 5, 10, 20, and 30 cm in water. The dose enhancement factor (DEF) and the energy fluence were obtained by Monte Carlo calculations of the particle and heavy ion transport code system (PHITS).

Results: The DEFs at the centre of Lipiodol with the FF beam were 6.8, 7.3, 7.6, 7.2, 6.1, and 5.7% and those with the FFF beam were 20.6, 22.0, 21.9, 20.0, 12.3, and 12.1% at depths of 1, 3, 5, 10, 20, and 30 cm, respectively, where Lipiodol was located in water. Moreover, spectrum results showed that more low-energy photons and electrons were present at shallow depth where Lipiodol was located in water. The variation in the low-energy spectrum due to the depth of the Lipiodol position was more explicit with the FFF beam than that with the FF beam.

* Corresponding author at: Radiation Therapy Section, Department of Clinical Support, Hiroshima University Hospital, 1-2-3 Kasumi, Minami-ku, Hiroshima City 734-8551, Japan.

E-mail address: daika99@hiroshima-u.ac.jp (D. Kawahara).

<https://doi.org/10.1016/j.rpor.2017.12.004>

1507-1367/© 2018 Greater Poland Cancer Centre. Published by Elsevier Sp. z o.o. All rights reserved.

Conclusions: The current study revealed variations in the DEF and energy spectrum due to the depth of the Lipiodol position with the FF and FFF beams. Although the FF beam could reduce the effect of energy dependence due to the depth of the Lipiodol position, the dose enhancement was overall small. To cause a large dose enhancement, the FFF beam with the distance of the patient surface to Lipiodol within 10 cm should be used.

© 2018 Greater Poland Cancer Centre. Published by Elsevier Sp. z o.o. All rights reserved.

1. Introduction

Stereotactic body radiation therapy (SBRT) delivers high-dose radiation to hepatocellular carcinoma (HCC). Although the SBRT procedure and treatment evaluation varies in different facilities, the ability and safety of this technique for intra-hepatic HCC has been reported.¹ In the liver, when Lipiodol is used as an embolic agent, SBRT can be used for tumour seeking in trans arterial chemoembolization (TACE).² Recently, promising responses in patients with unresectable hepatocellular carcinoma treated with TACE followed by radiation therapy have been reported.^{2,3} In our previous study, we reported the dose enhancement in Lipiodol,⁴ where only the absorbed dose at the depth of 5.0 cm was considered using Lipiodol located in a water-equivalent phantom ($3 \times 3 \times 3 \text{ cm}^3$). The dose enhancement was 6.0% with a 10 MV FFF beam for the clinical case. However, the difference in the dose enhancement with the FF and FFF beams, variations in dose enhancement due to the depth of the Lipiodol position, and difference in the energy spectra were not investigated.

The Varian TrueBeam linear accelerator can produce flattened (FF) and flattening-filter-free (FFF) beams. While it is advantageous to use an FFF beam in radiation dose delivery, the removal of the flattening filter significantly decreases the beam attenuation and increases the photon fluence. Thus, it also affects the photon energy distribution or beam quality.^{5,6} For the FFF beam, these low-energy photons contribute to dose deposition in the photon-beam build-up region close to the patient surface. Compared to the FF beam, although the FFF beam has smaller head scattering and leakage, measurements and Monte Carlo (MC) simulations found that irradiation of the FFF beam results in a higher surface dose than the FF beam.⁷ This indicates that low-energy photons may play an important role in the surface dose enhancement of the FFF beam. Therefore, it is worthwhile to evaluate the difference in dose enhancement due to the depth, where Lipiodol was located, using FF and FFF beams.

The purpose of this study is twofold: (i) to evaluate the dose enhancement and (ii) to investigate the energy spectrum variations of photons and electrons at various depths due to the depth of the Lipiodol position with FF and FFF beams.

2. Methods and materials

2.1. Linac and Monte Carlo calculation

A TrueBeam linear accelerator (linac) (Varian Medical Systems, Palo Alto, USA) provides FFF and FF beams of 6 MV was used.

BEAMnrc and PHITS-based MC scripts were used to model the linac. Geant4 and EGSnrc are the most widely used tools in medical physics.^{8,9} An important special-purpose code built on the EGSnrc platform is the user code BEAMnrc.¹⁰ This code is optimized to model the treatment head of radiotherapy linacs and includes a number of geometry and source subroutines, together with variance reduction techniques to enhance the efficiency of simulations.¹¹ Phase space files were created in two stages because the components of the TrueBeam accelerator head are proprietary and not available to the public for direct simulations. The first stage of the phase space files located just above the secondary X/Y collimator was simulated using the GEANT4 MC code and provided IAEA-compliant phase-space files by Varian. Using the first stage of the phase space files, the second stage of the phase space files located below the secondary collimator was modelled using the Beamnrc MC code. The second phase-space data scored at a source-to-surface distance (SSD) of 70 cm were used as input data for an inhomogeneity virtual phantom. Although BEAMnrc can easily create the linac model, BEAMnrc cannot analyze the energy spectrum in the phantom. PHITS can deal with the transport of nearly all particles, including neutrons, protons, heavy ions, photons, and electrons, over wide energy ranges using several nuclear reaction models and nuclear data libraries. There were some studies about the energy spectrum for linacs with the PHITS code.¹² Thus, the dose calculation and photon and electron energy spectrum acquisitions were performed for water and the Lipiodol phantom using the PHITS code. The dose calculation grid size was 2.0 mm. The number of photon histories in Beamnrc and PHITS were 2.0×10^8 and 2.0×10^9 , respectively.

2.2. Evaluation of the dose enhancement factor

A virtual inhomogeneity phantom, with Lipiodol ($3 \times 3 \times 3 \text{ cm}^3$) located on the central axis at depths of 1, 3, 5, 10, 20, and 30 cm in a water-equivalent phantom ($40 \times 40 \times 40 \text{ cm}^3$) was made (Fig. 1). Lipiodol contains 480 mg/mL of Iodine organically combined with ethyl esters of fatty acids of poppy seed oil. The mass density of Lipiodol was overridden by 1.28 g/cm^3 . A field size of $5 \times 5 \text{ cm}^2$ was used for irradiation. In this field size, losses in longitudinal and lateral charged particle equilibrium could be small. The factors include the following, the electron range could be small in a high-Z and high-density material, and the effect of scattering in the lateral direction was within 0.5 cm in our previous study.⁴ The percent depth dose (PDD) curves were measured and normalized to the calculated dose at d_{max} . The DEF was estimated according to the following definition: the

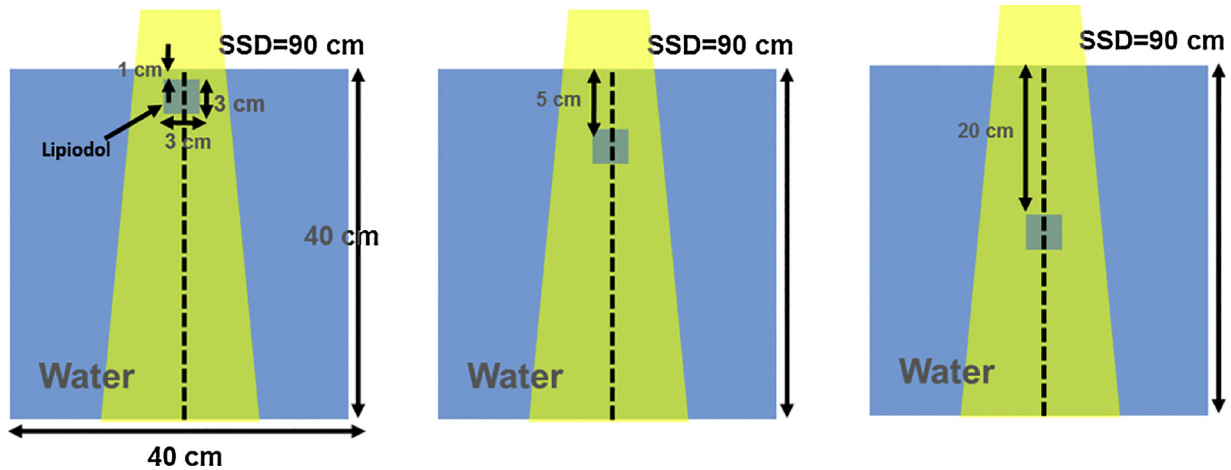


Fig. 1 – Geometric scheme of Lipiodol ($3 \times 3 \times 3 \text{ cm}^3$) located at depths of 1 cm (left), 5.0 cm (centre), and 20 cm (right) in a water-equivalent phantom ($40 \times 40 \times 40 \text{ cm}^3$).

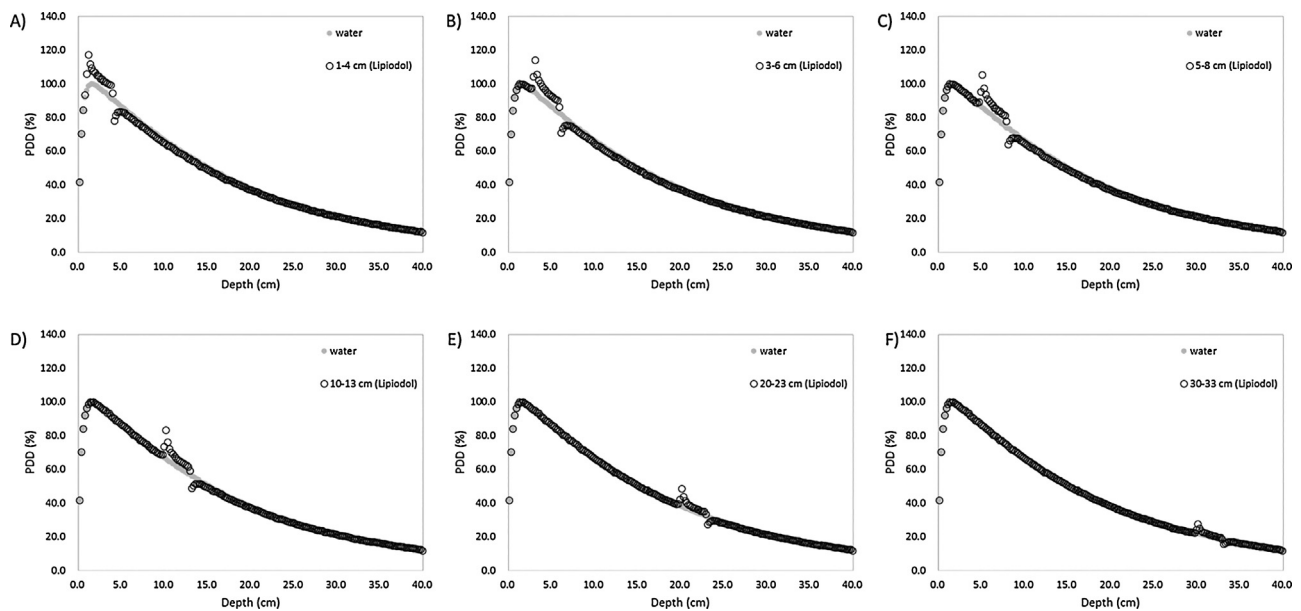


Fig. 2 – PDD curves for the virtual phantom with (open circles) and without (closed circles) Lipiodol at 1 cm (A), 3 cm (B), 5 cm (C), 10 cm (D), 20 cm (E), and 30 cm (F) with the FF beam.

deviation of the dose with the presence of Lipiodol and that without Lipiodol divided by the dose without Lipiodol.

2.3. Evaluation of energy spectrum variations of photons and electrons using a virtual phantom

Energy spectrum variations of photons and electrons were investigated using the same beam and virtual phantom (Section B). The number of bins in each spectrum was set to 50, logarithmically spaced with an energy range from 0 to 20 MeV. To compare the FF and FFF beams for beam obliquity, the energy flux was analyzed at the centre of Lipiodol (2.5, 4.5, 6.5, 11.5, 21.5, and 31.5 cm). The energy spectrum was normalized using the normalized factor defined as the difference between the dose at d_{max} with the FF and FFF beams.

3. Results

3.1. Evaluation of the DEF

Figs. 2 and 3 show the PDD curves calculated in the water phantom with and without Lipiodol using the FFF and FF beams by MC, respectively. All the PDDs were normalized to 100% at d_{max} for each beam. Fig. 4 shows the DEFs at the centre of Lipiodol with the FF and FFF beams. The DEFs at the centre of Lipiodol with the FF beam were 6.8, 7.3, 7.6, 7.2, 6.1, and 5.7% and those with the FFF beam were 20.6, 22.0, 21.9, 20.0, 12.3, and 12.1% at depths of 1, 3, 5, 10, 20, and 30 cm, respectively, where Lipiodol was located in water. The DEFs at depths larger than a Lipiodol position of 10 cm were decreased for both the FFF and FF beams. The DEFs with the FFF beam

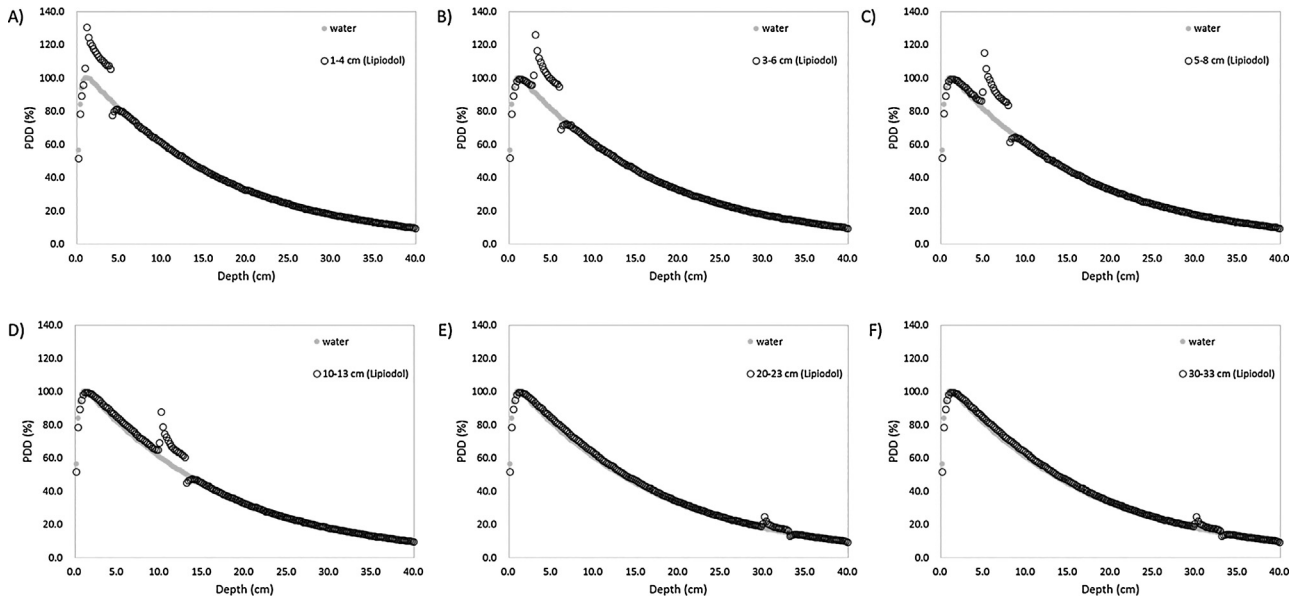


Fig. 3 – PDD curves for the virtual phantom with (open circles) and without (closed circles) Lipiodol at 1 cm (A), 3 cm (B), 5 cm (C), 10 cm (D), 20 cm (E), and 30 cm (F) with the FFF beam.

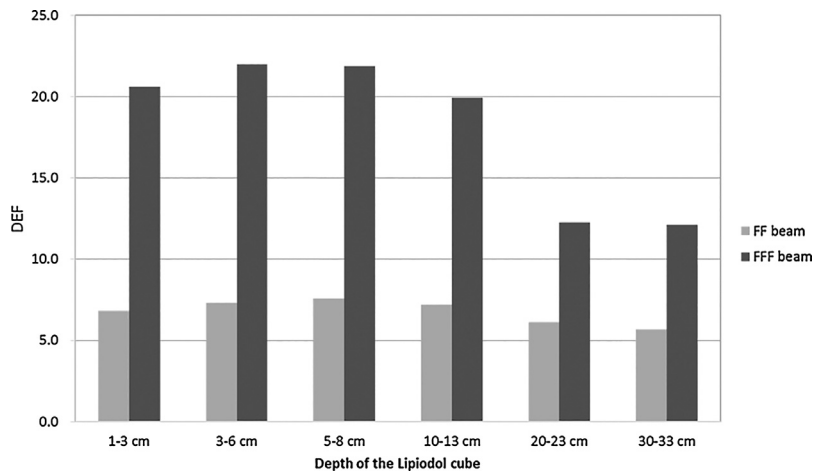


Fig. 4 – DEFs at the centre of Lipiodol with the FF (a) and FFF (b) beams.

were significantly larger than those with the FF beam at all depths.

3.2. Evaluation of the energy spectral variations of photon and electron with a virtual phantom

Figs. 5 and 6 show the distribution of the photon and electron energy fluence and energy of the FF and FFF beams, respectively. The energy spectra of photons and electrons are normalized to the maximum intensity. More low-energy photons in the ranges of 0.03–0.04 MeV and 0.06–1.5 MeV were contained. The FFF beam contained greater number of photons, mostly concentrated in the low-energy ranges of 0.03–0.04 MeV and 0.06–1.5 MeV as compared to the FF beam. More low-energy electrons in the range of 0–0.6 MeV were present at shallower depths of the Lipiodol position. Figs. 7 and 8 show the distribution of the photon and electron energy fluence and energy of the FF and FFF beams, which

were normalized at each energy bin of 30 cm depth to reveal the energy spectrum variations of photons and electrons due to the depth of the Lipiodol position at each energy bin. The difference in the photon energy spectrum in the low-energy ranges of 0.03–0.04 MeV and 0.06–1.5 MeV due to the depth of Lipiodol increased as the depth of Lipiodol decreased. The difference in the electron energy spectrum in the low-energy range of 0–0.6 MeV due to the depth of Lipiodol increased as the depth of Lipiodol decreased. The difference in the photon and electron energy fluence due to the depth of Lipiodol with the FFF beam increased compared to that with the FF beam.

4. Discussion

In a previous study, the surface dose difference was investigated using FFF and FF beams.^{13,14} They reported that the FFF beam had slightly higher surface dose in the build-up region

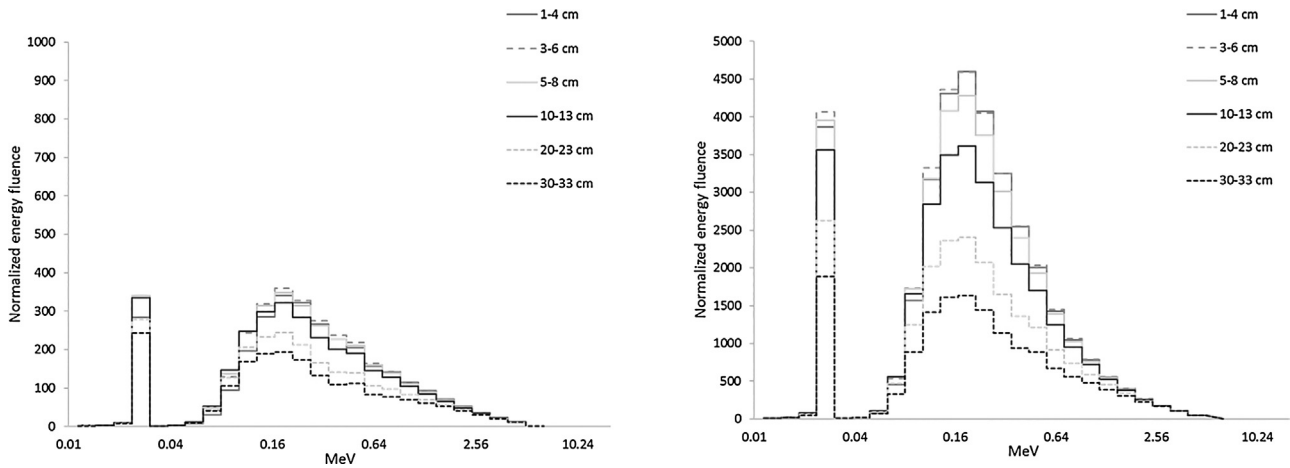


Fig. 5 – Photon energy fluence with the FF beam (left) and the FFF beam (right). The energy spectrum of photons is normalized to the maximum intensity.

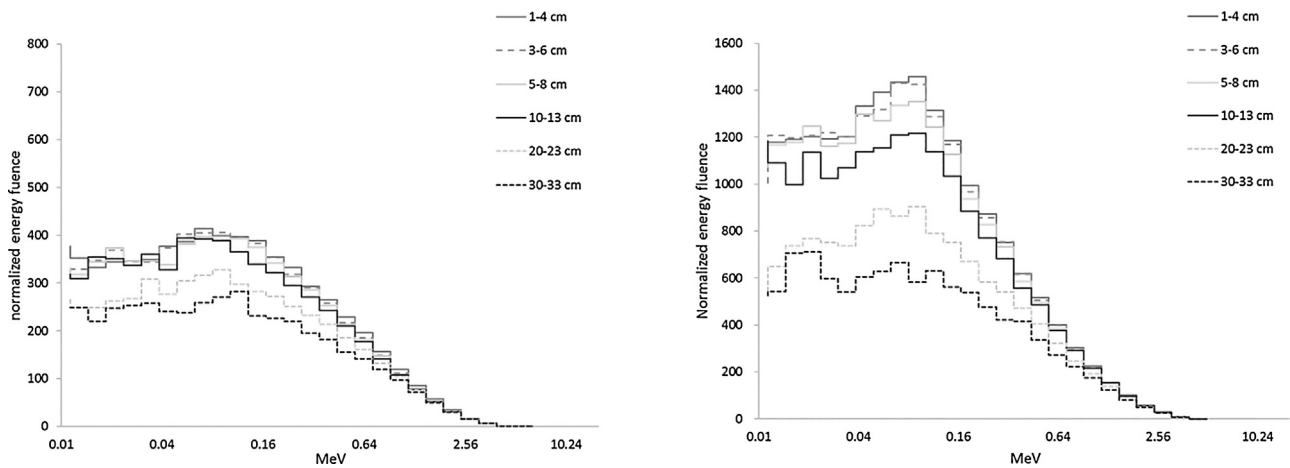


Fig. 6 – Electron energy fluence with the FF beam (left) and the FFF beam (right). The energy spectrum of electrons is normalized to the maximum intensity.

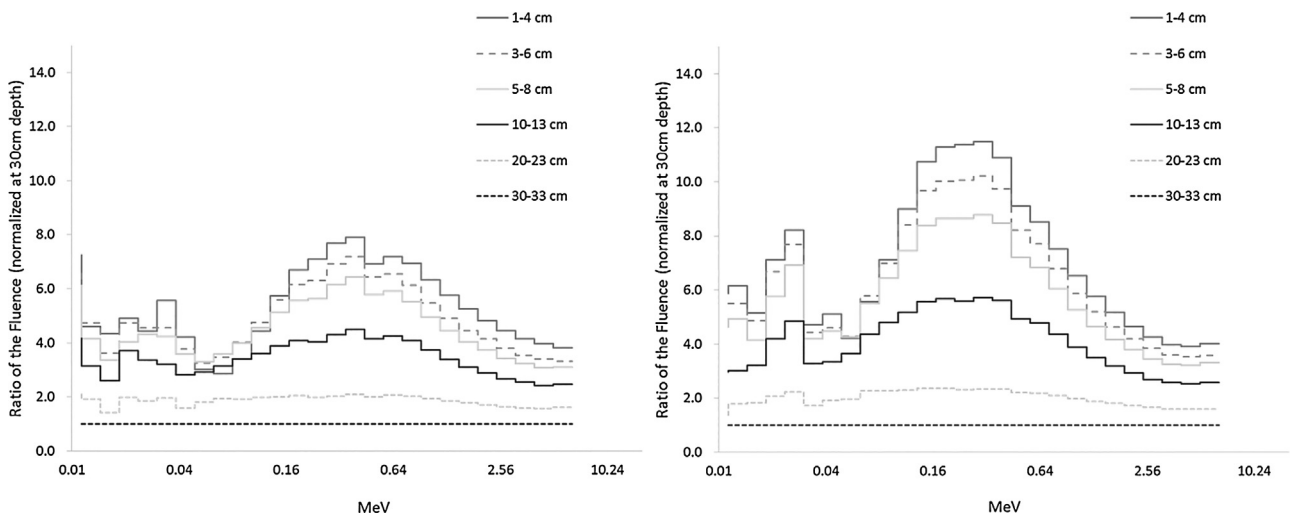


Fig. 7 – Photon energy fluence with the FF beam (left) and the FFF beam (right). The energy spectrum of photons is normalized at each energy bin of a depth of 30 cm.

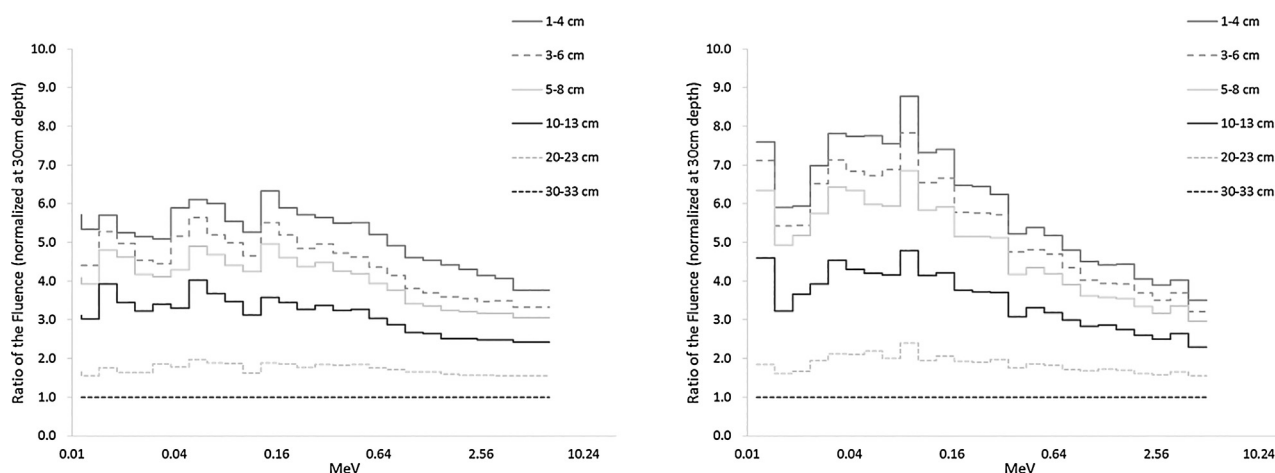


Fig. 8 – Electron energy flux with the FF beam (left) and the FFF beam (right). The energy spectrum of electrons is normalized at each energy bin of a depth of 30 cm.

than the corresponding FF beam for a field size $\leq 10 \times 10 \text{ cm}^2$. They showed that the FFF beam contained more low-energy photons in the build-up region. In our study, the same trend was observed, where the FFF beam contained more low-energy photons (0.03–0.04 MeV and 0.06–1.5 MeV), as shown in Fig. 5. The difference of the photon and electron energy spectra between the FF and FFF beams was affected owing to beam hardening by a flattening filter. Plato showed the difference in the DEFs and energy spectra with the FF and FFF beams as a function of the off-axis distance in water phantoms.¹⁵ However, Plato did not evaluate the energy spectrum variations due to the depth. In the current study, we evaluated the variations in the DEF and the photon and electron energy spectrum due to the depth of the Lipiodol position. Although the difference between the DEF and the FFF beam due to the depth of Lipiodol at depths more than 10 cm of the Lipiodol position was within 2%, it was greater than 5% at depths larger than 20 cm of the Lipiodol position. This means that the distance of the patient surface to Lipiodol should be less than a Lipiodol depth of 10 cm with the FFF beam to cause higher dose enhancement. The number of low-energy photons and electrons with the FFF beam decreased as the depth of the Lipiodol position increased. In the photon energy spectrum, more low-energy photons were contained at shallow depths, as shown in Figs. 5 and 6. Sarah et al. reported that the average photon energy is higher when approaching the surface depth.¹⁶ This suggests that low-energy photons affect the dose enhancement, and the amount of low-energy photons was significantly decreased owing to the depth. Nevertheless, the difference of the DEF with the FF beam was due to the depth of Lipiodol at depths greater than a Lipiodol position of 30 cm was within 1.9%. The difference due to the depth of the Lipiodol position of the number of photons and electrons with the FF beam was small. Clinically, although the dependence of the depth of the Lipiodol position for the FF beam was small, the dose enhancement was overall small. However, for the FFF beam, the dose enhancement was large when the distance of the patient surface to Lipiodol was short.

The limitation of our study is that the arrangement of Lipiodol molecules and tumour cells on the CT image was

not considered. A previous study reported that photon source energy and the size of Au nanoparticles (AuNPs), which was a high-density material such as iodine, influence the spatial distribution of the energy deposited around AuNPs.¹⁷ It was suggested that electrons lose their energy over a larger distance and can cross-fire between cells; however, they can still cause significant DNA damage. The effect depends mostly on the energy spectrum of incident photons, with more energetic photons yielding higher energy and longer-range photoelectrons. Thus, the energy of secondary electrons is likely to be sufficiently high to enable cross-firing between tumour cells in the proximity of Lipiodol molecules. Therefore, the dose to these tumour cells can be assumed to be almost equal to the dose delivered to Lipiodol.

5. Conclusion

The current study revealed variations in the DEF and the energy spectrum due to the depth of the Lipiodol position with the FF and FFF beam. Although the FF beam could reduce the effect of energy dependence due to the depth of the Lipiodol position, the dose enhancement was overall small. To cause large dose enhancement, the FFF beam with the distance of the patient surface to Lipiodol within 10 cm should be used.

Conflict of interest

None declared.

Financial disclosure

This work was supported by the Foundation of Cancer Research in Japan.

REFERENCES

1. Dawson LA, Jaffray DA. Advances in image-guided radiationtherapy. *J Clin Oncol* 2007;25:938–46;

- Chang JY, Balter PA, Dong L, et al. Stereotactic body radiation therapy in centrally and superiorly located stage I or isolated recurrent non-small-cell lung cancer. *Int J Radiat Oncol Biol Phys* 2008;**72**:967–71.
2. Li B, Yu J, Wang L, et al. Study of local three dimensional conformal radiotherapy combined with transcatheter arterial chemoembolization for patients with stage III hepatocellular carcinoma. *Am J Clin Oncol* 2003;**26**:e92–9.
 3. Ishikura S, Ogino T, Furuse J, et al. Radiotherapy after transcatheter arterial chemoembolization for patients with hepatocellular carcinoma and portal vein tumor thrombus. *Am J Clin Oncol* 2002;**25**:189–93; Hawkins MA, Brock KK, Eccles C, et al. Assessment of residual error in liver position using kV cone-beam computed tomography for liver cancer high-precision radiation therapy. *Int J Radiat Oncol Biol Phys* 2006;**66**:610–9.
 4. Kawahara D, Oawa S, Saito A, et al. Dosimetric impact of Lipiodol in stereotactic body radiation therapy on liver after trans-arterial chemoembolization. *Med Phys* 2017;**44**(Jan (1)):342–8.
 5. Sixel KE, Faddegon BA. Calculation of X-ray spectra for radiosurgical beams. *Med Phys* 1995;**22**:1657–66.
 6. Titt U, Vassiliev ON, Ponisch F, Dong L, Liu H, Mohan R. A flattening filter free photon treatment concept evaluation with Monte Carlo. *Med Phys* 2006;**33**:1595–602.
 7. Wang Y, Khan MK, Ting JY, Easterling SB. Surface dose investigation of the flattening filter-free photon beams. *Int J Radiat Oncol Biol Phys* 2011;**83**:281–5.
 8. Parsons D, Robar JL, Sawkey D. A Monte Carlo investigation of low-Z target image quality generated in a linear accelerator using Varian's VirtualLinac. *Med Phys* 2014;**41**(Feb (2)):021719.
 9. Kawrakow I, Mainegra-Hing E, Rogers DWO, Tessier F, Walters BRB, National Research Council of Canada Report PIRS-701 *The EGSnrc code system: Monte Carlo simulation of electron and photon transport*. Ottawa, Canada: NRCC; 2013.
 10. Rogers DW, Walters B, Kawrakow I, National Research Council of Canada Report PIRS-0509(A) revL *BEAMnrc users manual*. Ottawa, Canada: NRCC; 2016.
 11. Rogers DW, Faddegon BA, Ding GX, Ma CM, We J, Mackie TR. BEAM: a Monte Carlo code to simulate radiotherapy treatment units. *Med Phys* 1995;**22**(5):503–24.
 12. Puchalska M, Sihver L. PHITS simulations of absorbed dose out-of-field and neutron energy spectra for ELEKTA SL25 medical linear accelerator. *Phys Med Biol* 2015;**60**(Jun (12)):N261–70.
 13. Cashmore J. Surface dose variations in 6 and 10 MV flattened and flattening filter-free (FFF) photon beams. *J Appl Clin Med Phys* 2016 Sep 8;**17**(5):293–307.
 14. Wang Y, Khan MK, Ting JY, Easterling SB. Surface dose investigation of the flattening filter-free photon beams. *Int J Radiat Oncol Biol Phys* 2012;**83**:281–5.
 15. Lee PC. Monte Carlo simulations of the differential beam hardening effect of a flattening filter on a therapeutic X-ray beam. *Med Phys* 1997;**24**(Sep (9)):1485–9.
 16. Scarboro SB, Followill DS, Howell RM, Kry SF. Variations in photon energy spectra of a 6 MV beam and their impact on TLD response. *Med Phys* 2011;**38**(May (5)):2619–28.
 17. Lechtman E, Chattopadhyay N, Cai Z, Mashouf S, Reilly R, Pignol JP. Implications on clinical scenario of gold nanoparticle radiosensitization in regards to photon energy, nanoparticle size, concentration and location. *Phys Med Biol* 2011;**56**(15):4631–47.